Classification: BIOLOGICAL SCIENCES

Title: Evolutionary tipping points in the capacity to adapt to environmental change

Authors: Carlos A. Botero[1]*, Franz J. Weissing[2], Jonathan Wright[3] and Dustin R. Rubenstein[4]

Affiliations:

[1] Initiative for Biological Complexity and the Department of the Interior Southeast Climate Science Center, North Carolina State University, Raleigh NC, 27695, USA; Department of Biology, Washington University in St. Louis, St. Louis MO, 63130, USA.

[2] Centre for Ecological and Evolutionary Studies, University of Groningen, Nijenborgh 7, 9747 AG Groningen, The Netherlands

[3] Centre for Biodiversity Dynamics, Department of Biology, Norwegian University of Science and Technology (NTNU), NO-7491, Trondheim, Norway.

[4] Department of Ecology, Evolution and Environmental Biology, Columbia University, 10th Floor Schermerhorn Extension, 1200 Amsterdam Avenue, New York, NY 10027, USA.

*** Correspondence to:** cabotero@ncsu.edu, T: 919-943-7969

Keywords: Fluctuating selection, Global change, Phenotypic plasticity, Bet-hedging, Adaptive tracking.

Abstract

In an era of rapid climate change there is a pressing need to understand how organisms will cope with faster and less predictable variation in environmental conditions. Here we develop a unifying model that predicts evolutionary responses to environmentally driven fluctuating selection, and use this theoretical framework to explore the potential consequences of altered environmental cycles. We first show that the parameter space determined by different combinations of predictability and timescale of environmental variation is partitioned into distinct regions where a single mode of response (reversible phenotypic plasticity, irreversible phenotypic plasticity, bet-hedging, or adaptive tracking) has a clear selective advantage over all others. We then demonstrate that although significant environmental changes within these regions can be accommodated by evolution, most changes that involve transitions between regions result in rapid population collapse and often extinction. Thus, the boundaries between response mode regions in our model correspond to 'evolutionary tipping points' where even minor changes in environmental parameters can have dramatic and disproportionate consequences on population viability. Finally, we discuss how different life histories and genetic architectures may influence the location of tipping points in parameter space and the likelihood of extinction during such transitions. These insights can help identify and address some of the cryptic threats to natural populations that are likely to result from any natural or human-induced change in environmental conditions. They also demonstrate the potential value of evolutionary thinking in the study of global climate change.

Significance statement: Environmental variation is becoming more frequent and unpredictable as a consequence of climate change, yet we currently lack the tools to evaluate the extent to which organisms may adapt to this phenomenon. Here we develop a model that explores these issues and use it to study how changes in the timescale and predictability of environmental variation may ultimately affect population viability. Our model indicates that although populations can often cope with fairly large changes in these environmental parameters, on occasion they will collapse abruptly and go extinct. We characterize the conditions under which these 'evolutionary tipping points' occur and discuss how vulnerability to such cryptic threats may depend on the genetic architecture and life history of the organisms involved.

/body

Introduction

Understanding how organisms cope with and adapt to changes in their environments is a central theme in evolutionary ecology (1). However, we currently lack the tools to predict the most likely evolutionary responses to changes in environmental conditions (see (2)), including those currently experienced through global change (3, 4). Evolutionary responses to within- and among-year fluctuation in ecological parameters like ambient temperature or precipitation can be highly informative about the process of adaptation to environmental change, as well as about the potential consequences of the recently accelerated rates of environmental change and the associated increase in climatic variability and unpredictability (5-8). Earlier work indicates that some organisms face environmental uncertainty by hedging their bets with a strategy that minimizes fitness variance across all possible environmental conditions (conservative bet-

66 hedging (9)), while others have evolved a mix of strategies to take advantage of alternative
67 environmental scenarios in a probabilistic fashion (diversification bet-hedging (9)). In still other
68 cases, organisms cope with environmental variation through phenotypic plasticity, which is the
69 ability to respond to environmental cues through the adjustment of genotypic expression either
70 during early development (irreversible or developmental plasticity (10)) or throughout life
71 (reversible plasticity (11)). Finally, environmental variation is also known to result in correlated
72 variation in mean population traits, as natural selection favors different phenotypes over
73 evolutionary time (adaptive tracking (12)). Although an increasing amount of attention has been
74 recently devoted to the conditions that promote these different forms of evolutionary response to
75 environmental variation (hereafter 'response modes') (2, 9, 13-18), most studies have considered
76 only one or a small subset of response modes (16, 17), and few have explored the general
77 conditions under which one (or more) may be selected above the others (2, 18). Addressing these
78 issues will be critical for improving our ability to predict whether and how populations will adapt
79 to both natural and human-induced environmental change.

80 Here we develop a theoretical model that considers the joint evolution of a
81 comprehensive range of evolutionary responses to environmental variation. Although we
82 illustrate our model by exploring the effects of temperature, the principles we describe apply to
83 other naturally fluctuating environmental variables (e.g., precipitation). We use the term
84 'insulation', I, as a broad descriptor of morphological (e.g., coat thickness (19)), behavioral (e.g.,
85 huddling), or physiological (e.g., sweating) characteristics that help counter thermal stress. To
86 investigate the dynamics of adaptation to environmental variation, we use individual-based
87 evolutionary simulations in which the pattern of variation in genotypic expression across a range
88 of environmental conditions (i.e., the reaction norm of the genotype (14)) is assumed to be

heritable and subject to mutation and natural selection. We begin by testing the consistency of evolutionary response to different types of environmental change and then use this general framework to explore how systems react to disruption in the nature of environmental oscillations. A non-technical description of how our model can inform issues related to global change is included in the SI text.

Results

Environmental variation includes both deterministic (i.e., climate) and stochastic (i.e., weather) components. For example, temperatures oscillate deterministically from cold winters to hot summers, but the actual values experienced in a given day vary stochastically from the seasonally expected average. We modeled these components as

$$E_t = A \cdot \sin\left(2\pi t / LR\right) + B \cdot \varepsilon,$$

where t is time, L is the number of time steps per generation (i.e., lifespan), R is the relative timescale of environmental variation (i.e., number of generations per environmental cycle), ε is a stochastic error term, and A and B are scaling constants reflecting the relative importance of deterministic and stochastic factors. This equation describes a simple sinusoidal oscillation in environmental conditions when R is intermediate or small, and approximates a slow directional change when R is very large. Because R is a relative metric, the findings presented below are easily applicable to organisms with different lifespans.

In nature, changes in environmental conditions are often preceded by correlated changes in photoperiod, barometric pressure, or other environmental cues. For example, day length variation tends to be well correlated with seasonal temperature variation in temperate regions. Thus, we model the predictability of environmental conditions, P, by altering the degree to

112 which an environmental cue, C, is correlated with future temperature values (see SI text and Fig.
113 S1). When temperatures and cues are perfectly correlated, the environment is completely
114 predictable, $P = 1$, and when they are not correlated at all, it is completely unpredictable, $P = 0$.
115 In the simulations presented here, cues are provided to individuals prior to experiencing any
116 changes in their environment (see Methods).

117 Simulation runs in our model proceed in discrete time steps with non-overlapping
118 generations and individual lifespans of $L = 5$ time steps. Individuals possess seven genetic traits
119 – loci h, s, a, I_0, I_0', b and b' – that determine the amount of insulation to be produced under
120 different environmental cues. Every genotype specifies two different reaction norms: one
121 encoded by I_0 and b, and another one encoded by I_0' and b'. Loci I_0 and I_0' determine baseline
122 degrees of insulation whereas loci b and b' determine the degree to which insulation is made
123 dependent on environmental cues. Each individual in our model expresses only one of these
124 reaction norms through life: the one based on I_0 and b is chosen at birth with probability h,
125 whereas the one based on I_0' and b' is chosen with probability 1-h. In practice, this implies that
126 locus h enables individuals with the same genotype to respond to environmental variation in two
127 completely different ways (as in diversifying bet-hedging). Locus s is a genetic switch that
128 determines whether the organism makes its insulation dependent on environmental cues (i.e.,
129 whether it allows for phenotypic plasticity; $s > 0.5$) or not ($s \leq 0.5$). Non-plastic individuals
130 ignore environmental cues and exhibit a fixed insulation phenotype encoded by the baseline loci
131 I_0 or I_0'. Plastic individuals adjust their insulation phenotypes, I, to the environmental cues they
132 perceive using linear norms of reaction such that, $I = I_0 + b \cdot C$ or $I = I_0' + b' \cdot C$. Locus a
133 determines whether this cue-dependence is only happening during ontogeny (irreversible or
134 developmental plasticity) or also throughout the individual's lifetime (reversible phenotypic

plasticity). In practice, this means that individuals with $a = 0$ respond to environmental cues only during development—and therefore exhibit a single phenotype throughout life — whereas those with $a > 0$, alter their phenotypes with probability a at each time step after development. As in earlier studies (14), we assume that phenotypic plasticity is costly both during and after development. Thus, plastic individuals pay a one-time developmental cost, k_d, and each phenotypic adjustment after development is assumed to incur in an additional cost of k_a.

To establish a baseline for comparison, we began by evaluating the effects of environments with a constant temperature. As expected, this simple scenario led to the evolution of non-plastic insulation strategies with a mean population value that approximately matched the temperature experienced. We then considered completely stochastic environments ($A = 0$ and $B = 1$), where individuals had no information about the potential state of the environment ($P = 0$). Under these conditions, populations evolved to ignore uninformative cues, producing instead a fixed phenotype at the average environmental condition ($I = 0$, Fig. 1A). In contrast, when we allowed these same stochastic environments to be completely predictable ($P = 1$), the resulting reaction norms led to insulation levels that varied with the intensity of environmental cues (Fig. 1B). In completely deterministic environments ($A = 1$ and $B = 0$) with rapid environmental variation ($\log R = 0$), we observed that phenotypic plasticity also evolved only when individuals were able to anticipate environmental changes (Figs. 1C and 1D). This result highlights a key aspect of adaptation to environmental change: the way in which environments vary (i.e., whether the pattern of environmental oscillations appears to be stochastic or deterministic) is less important to evolution than the degree to which individuals can anticipate the future state of the environment (21). Thus, the remaining simulations focus on the effects of predictability of environmental variation and assume, for simplicity, that $A = 1$ and $B = 0$ (see SI text).

We proceeded to explore evolutionary outcomes at different predictability levels and across a comprehensive range of timescales of variation (Fig. 2). For each set of conditions, we performed 100 replicated simulations. Each subplot in Fig. 2A depicts the 100 evolved mean reaction norms at generation 50,000 (e.g., $I = \bar{b} \cdot C + \overline{I_0}$, where $\bar{b}$ and $\overline{I_0}$ correspond to the mean population values for b and I_0). Overall, we find that evolution results in remarkably consistent outcomes for the majority of parameter combinations (Fig. 2A, SI text and Fig. S2) and that different response modes occur largely in non-overlapping regions of parameter space (Fig. 2B, Table S1, SI Text and Fig. S3). These findings are robust to the implementation of density- and frequency-dependent selection, as well as to alternative coding schemes for genotype-to-phenotype mapping (SI text and Fig. S4). In cases where environmental variation within a generation is both predictable and fast (P is large, R is small; upper left corner of Fig. 2B), each subplot in Fig. 2A shows a single cluster of reaction norms. This indicates that (i) similar reaction norms evolved in all 100 replicate simulations at that parameter combination, (ii) the evolved populations exhibit a high degree of plasticity (i.e., $\bar{s} > 0.5$ and $\bar{b} \approx 1$), and (iii) individuals in these populations often adjust their phenotypes after development ($\bar{a} \approx 1$, see 'reversible plasticity' in Table S1). As R becomes larger, locus a quickly evolves to $\bar{a} \approx 0$ (depicted in blue in Fig. 2A) because the diminishing benefits of avoiding thermal mismatches no longer surpass the costs of phenotypic adjustment (13, 22, 23). We label this strategy 'irreversible plasticity' because individuals in these populations exhibit plasticity exclusively during development. The transition from reversible to irreversible plasticity occurs at progressively shorter timescales in less predictable environments because the expected benefits of phenotypic adjustment decrease with higher potential for errors in anticipating environmental change.

When environmental conditions are fairly unpredictable, the rate at which environments change determines the resulting evolutionary outcome (Figs. 2 and 3). If R is large (lower right corner of Fig. 2B), the slow rate of environmental change allows for beneficial mutations in I_0 to appear and approach fixation. The resulting pattern is a gradual change of the mean phenotype that tends to lag behind the change in environmental conditions ('adaptive tracking' in Fig. 3A). However, at faster timescales (lower center and lower left in Fig. 2B), environmental change is too fast to be tracked by mutation and too unpredictable to be addressed through plasticity. Consistent with previous studies (9, 16), this extreme form of uncertainty forces individuals to hedge their bets. When individuals experience all possible conditions with similar probability (e.g., very low R), we observe the evolution of fixed phenotypes at $I \approx 0$. Although this insulation value rarely matches the actual conditions experienced, it matches the average environment and therefore minimizes overall thermal mismatch across the entire range of potential environmental conditions (Table S1). Thus, this strategy resembles conservative bet-hedging (9) in that it minimizes the variance in fitness among selection events and across individuals that share the same genotype. In contrast, when individuals of a given genotype experience only a fraction of the environmental cycle (e.g., $\log R = 0.5$), we observe the evolution of mixed-strategies that produce alternative phenotypes with either heavy or light insulation in a probabilistic fashion (green in Fig. 2A). This strategy resembles the phenotypic polymorphism of diversification bet-hedging (9) (Table S1), because the different phenotypes produced by a single genotype minimize thermal mismatch in different scenarios (i.e., the larger I phenotype does best when experiencing disproportionally more of the upper than the lower half of the environmental cycle, and the smaller I phenotype does best in the opposite situation).

Having determined the most likely evolutionary outcomes under a comprehensive range of parameter combinations, we proceeded to explore how populations are affected by changes in the predictability or timescale of environmental variation (i.e., in the 'signature' of their environment). The well-defined response mode regions observed in Fig. 2 allowed us to make a simple but important *a priori* prediction: changes in environmental signatures that require the evolution of an entirely different mode of response may be harder to cope with than those that do not. To test this hypothesis we abandoned the assumption of a constant population size in our model and linked reproductive output to absolute rather than relative fitness (see Methods). By relaxing this assumption, we were able to assess the demographic consequences (e.g., changes in population size and risk of extinction) of different environmental challenges. In this eco-evolutionary version of our model, maximal fecundity, q, was defined as the average number of offspring that an individual produces when it pays no plasticity costs and is able to exactly match its environment at every time step of its life. Thus, the mean fecundity of individual i, $\overline{F}_i$, is determined by the fraction of the maximum payoff that it is able to achieve, such that $\overline{F}_i = q \cdot W_i / W_{\max}$ (see Methods). Fig. 4 depicts the potential for extinction at each parameter combination (inner squares) as well as during transitions between adjacent combinations in parameter space when $q = 2.2$ (see Fig. S5 for alternative values of q). Each of the four possible transitions to an adjacent cell is depicted using trapezoids. For example, the color of the upper trapezoid within a given subplot indicates the effects of transitioning from that particular parameter combination to the one above it. As predicted, we found that the potential for extinction during these transitions is considerably higher when populations are forced into a different response mode region (a result that holds even if much larger changes in P or R are attempted).

226 The non-uniformity of transitional extinction rates in our model is driven by at least two
227 different mechanisms. First, some transitions imply moving into regions of parameter space that
228 are particularly challenging for adaptation. For example, when environmental oscillations are
229 quick and unpredictable (i.e., the bet-hedging region), baseline levels of extinction are high,
230 particularly at lower q values (see Fig. S5). Thus, any population that is suddenly forced into this
231 region will also be expected to have a high likelihood of extinction (Fig. 4A). The second
232 contributor to extinction relates to the complexity of genetic changes required for adaptation
233 during transition and is more readily observable after accounting for potential differences in
234 baseline levels of extinction in the new environments. For example, when relative extinction
235 rates are considered (Fig. 4B), we find that extinction is only more likely than expected when
236 populations move into a different response mode region (even if this transition involves moving
237 into regions of parameter space that appear to be easier for adaptation, such as into more
238 predictable environments). The reason for the increased risk of extinction during these 'tipping
239 point transitions' is that adapting to a completely new strategy for phenotypic development often
240 requires a radical restructuring of the genome, which can be particularly difficult to achieve as
241 populations collapse (Fig. 5). For example, in the transition from phenotypic plasticity to bet-
242 hedging, plastic strategies become maladapted (i.e., their expected number of offspring, W, is
243 less than one) and population decline is swift (Fig. 5A). Thus, given that adaptation to the new
244 environment requires in this case resetting developmental switches (s and a) and adjusting
245 almost every other loci in the virtual genome, the stochastic nature of mutation supply and the
246 reduced standing genetic variation of declining populations are more likely to result in extinction
247 (Fig. 5A) than in evolutionary rescue (Fig. 5B). Conversely, the relative extinction rates for the
248 reverse transition are also high because the fitness of fixed strategies is low compared to that of

plastic ones, and because many of the mutations that can potentially transform a fixed strategy into a plastic one will, in the absence of other necessary genetic changes, result in maladapted phenotypes. Another case with high relative rates of extinction during tipping point transitions is the change from conservative to diversifying bet-hedging, which involves similarly extensive genetic changes, including the resetting of h, I_0, I_0', b and b'. In contrast, when genomic changes are relatively simple, as in the case of the transition between reversible and irreversible plasticity, the likelihood of adaptation during transition is much higher (Fig. 4).

Discussion

Our model suggests that evolutionary response to environmental variation may be more predictable than previously anticipated. Through evolutionary simulations we have shown that fundamentally different adaptive responses consistently evolve under different timescales and predictabilities of environmental variation. The response mode regions predicted by our model are largely consistent with a variety of empirical findings in a range of biological systems. For example, reversibly plastic adaptations like torpor (24) and hibernation (25) have been shown to occur in response to frequent (i.e., daily or yearly) and predictable changes in environmental conditions. In some examples of reversible phenotypic changes, such as the seasonal change in coat coloration in temperate mammals, there is even evidence that the increasing unpredictability of relevant environmental parameters is currently exerting strong selection on natural populations (e.g., snow cover for snowshoe hares (26)). Another potential example of reversibly plasticity is cognitive ability, particularly given its role in enabling behavioral flexibility (27). Consistent with our predictions, the evolution of cognitive enhancement appears to be driven in many systems by the exposure to intense, short-term, and only moderately predictable

environmental variation (28-30). In contrast, most well documented examples of developmental (i.e., irreversible) plasticity occur when environmental features remain constant during a lifetime but vary among individuals. For example, the short-lived *Daphnia cucullata*, only develops costly and life-long protective helmets if coexisting with predatory fish (31). Empirical examples of conservative (e.g., cooperative breeding behavior (32)), and diversifying bet-hedging (e.g., maternal adjustment of variance in offspring traits (33) or fimbriae expression in bacteria (34)), also conform to our predictions as they all involve responses to highly unpredictable environmental conditions. Over much longer timescales, where our model predicts adaptive tracking, we see congruence with empirical examples like the slow changes in breeding and migration dates in birds (35) or even the rise of arid-adapted African mammals—including hominids — in response to increased aridity in East Africa during the Pliocene and early Pleistocene (36).

A key insight from our model is that adaptive capacity to environmental change is likely to be subject to 'evolutionary tipping points' (37), where most environmental changes will be relatively innocuous but some — even very small ones — can have disproportionate and dramatic effects. Specifically, the potential for adaption to changes in the predictability or timescale of environmental change appears to depend more on the location of parameter space that populations are moving into, than on the magnitude of the change itself. For example, our simulations indicate that evolution can easily accommodate rather large changes in environmental signatures if the same general strategy for phenotypic expression is appropriate before and after the change. However, it also shows that populations will decline rapidly and tend to go extinct whenever they are forced into situations where their current strategy is no longer appropriate (i.e., when crossing boundaries into different response mode regions, Fig. 5).

These observations have important implications in the context of global climate change because they suggest that even species that appear to be coping well with current changes in environmental signatures (3) may become vulnerable to extinction if a tipping point is crossed. Thus, an empirical characterization of evolutionary tipping point dynamics could be of major importance for a better understanding of otherwise cryptic threats to natural populations and for a proper design and implementation of conservation strategies.

Several aspects of the natural history of an organism are likely to influence the location and intensity of tipping points in parameter space. For example, species that pay higher costs of plasticity may move across an evolutionary tipping point much sooner than others, because the boundaries between plastic and non-plastic response mode regions occur at higher predictability values when k_a and k_d increase (Fig. 2). Similarly, organisms with slow life histories that do not reproduce often or that produce low numbers of progeny during each breeding attempt (modeled here as low values of q), are likely to be more vulnerable to environmental oscillations and tipping point transitions because of their potentially lower supply of beneficial mutations and their decreased ability to rebound from population bottlenecks (Fig. S5). In addition, our model indicates that the potential for extinction during tipping point transitions depends critically on the genetic architecture of relevant traits (38), and in particular on the number or magnitude of mutations required to achieve the genotypic optimum for the new selection regime. For example, we expect that populations will be more likely to go extinct when the strategy that needs to be evolved requires either *de novo* evolution (or loss) of complex organs and structures, or a major re-adjustment of basic physiological/developmental pathways. Conversely, we expect lower vulnerability to extinction when the desired new strategy after transition is achievable through the evolution of simple genetic changes that do not interfere with major body plans.

In conclusion, our model provides a unifying theoretical framework for predicting evolutionary responses to environmental change (8) and leads to a series of testable predictions regarding organismal capacity to adapt to natural or human induced changes in the environment. These predictions can be tested through experimental evolution of microorganisms or through comparative analyses of populations or species distributed along a gradient of environmental variation. Ultimately, evolutionary models like the one we present here can aide in determining the specific type of adaptation that organisms may use to cope with specific environmental changes, thereby improving our understanding of how populations and species may respond to either global change or other type of environmental challenge.

Methods

Norms of reaction. The tendency of a genotype to be systematically expressed as different phenotypes across a range of environmental conditions is known as the genotype's norm of reaction. Our model assumes that the effects of heat and cold stress are symmetric and that selection favors phenotypes that match the environmental condition in which they are expressed (see '*Fitness*' below). These simplifying assumptions imply that if individuals have perfect information about the environment, then they can maximize their returns with $I = E$. Accordingly, we have parameterized reaction norms in our model as linear functions. Thus, $I = I_0 + b \cdot C$ (or $I = I'_0 + b' \cdot C$ with probability 1-h), where I_0 is the insulation level produced at $C = 0$ and b is a slope that determines the degree to which insulation levels change as a function of changes in environmental cues (for alternative genotype-phenotype mapping schemes se SI text and Fig. S3).

Fitness. Every individual in our model lives for $L = 5$ time steps. Each time step proceeds in a defined order. First, environmental conditions are updated and environmental cues are computed from E_t and P as described above. Then, individuals have access to the cue and are given the opportunity to develop or adjust their phenotype accordingly. Finally, individuals are exposed to selection by computing their phenotypic mismatch, M, with the condition experienced such that,

$$M_{i,t} = \left| E_t - I_{i,t} \right|,$$

where E_t is the current environmental state and $I_{i,t}$ is the individual's current phenotype. At the end of a generation, a non-plastic individual's lifetime payoff, W_i, is computed as a function of the sum total of phenotypic mismatches throughout life, such that

$$W_i = \exp\left(-\tau \cdot \sum_{t=0}^{L} M_{i,t} \right),$$

where τ is a constant that determines the strength of fitness decay as a function of total phenotypic mismatch. For plastic individuals (i.e., $s > 0.5$),

$$W_i = \exp\left(-\tau \cdot \sum_{t=0}^{L} M_{i,t} \right) - k_d - n \cdot k_a$$

where n is the total number of times an individual adjusts its phenotype during its lifetime.

Individual-based simulations. Our evolutionary model is based on populations of 5,000 individuals exposed to mutation and natural selection for 50,000 discrete, non-overlapping generations (simulation runs were replicated 100 times at each parameter combination). Reproduction occurs only at the end of each generation and is proportional to the payoffs accumulated during each individual's lifetime (W_i). Thus, the number of offspring for individual i is drawn from a Poisson distribution with mean $W_i / \overline{W}$, where $\overline{W}$ is the mean cumulative

361 payoff for that generation. As a consequence, the average number of offspring per individual is
362 equal to one and the size of the offspring population is very similar to that of the parent
363 population. To compensate for the occasional differences between these two population sizes, we
364 randomly removed or replicated offspring when needed to maintain a population of 5,000. All
365 offspring in our model inherit the alleles at each locus from their parents, with a per locus
366 mutation probability of $\mu = 0.001$ and mutational steps drawn from a normal distribution with a
367 mean of zero and a standard deviation of 0.05. The loci that encode slopes in the reaction norms
368 (b and b') and reversibility in plasticity (a) are only allowed to mutate if individuals are plastic
369 (i.e., when $s > 0.5$). Otherwise, these traits are set to zero and subsequently ignored unless s
370 evolves a value greater than 0.5.

371 *Simulating transitions to different regions of parameter space.* To include the possibility
372 of varying population sizes into our model, we replaced relative with absolute fitness so that
373 reproductive output was directly tied to how well individuals were able to match their
374 environment. To this end, we modified the algorithm of our basic model so that the number of
375 offspring for individual i was drawn from a Poisson distribution with mean $q \cdot W_i / W_{\max}$, where
376 $W_{\max}$ is the maximum possible payoff (i.e., the payoff an individual would accrue if it paid no
377 costs and were able to match the exact temperature of its environment every time step of its life).
378 To prevent population size from exploding in cases where fecundity was large, we applied an
379 upper boundary constraint in these simulations at a population carrying capacity of 5,000
380 individuals; because increasing carrying capacity did not change qualitatively our results, we
381 maintained the population size used in the constant population size simulations. We then took the
382 final population of each replicate simulation in Fig. 2 and allowed it to evolve under different
383 values of P and/or R for 1,000 additional generations. In transition simulations where R remained

the same, we simply extended the environmental cycle from the time it was left off at the end of the initial simulation. When R changed, we adjusted the phase of the new environmental cycle to prevent abrupt discontinuities in the direction or magnitude of E.

Parameter settings. All simulations reported above are based on the following parameters unless otherwise stated: $L = 5$, $k_d = 0.02$, $k_a = 0.01$, $\tau = 0.25$, and $q = 2.2$. In every replicate, with the exception of transition simulations, the starting population was initialized by setting $h = 1$ (i.e., assuming that genomes only code for one norm of reaction), and by drawing the remaining traits for each individual at random from uniform distributions on [0, 1] for a and s; [-1, 1] for I_0 and I_0'; and [-2, 2] for b and b'. Subsequent evolution was completely unbounded and determined solely by mutation and natural selection.

References

1. Parmesan C (2006) Ecological and evolutionary responses to recent climate change. *Annual Review of Ecology Evolution and Systematics,* Annual Review of Ecology Evolution and Systematics), Vol 37, pp 637-669.
2. Piersma T & van Gils JA (2010) *The Flexible Phenotype: A Body-Centred Integration of Ecology, Physiology, and Behaviour* (Oxford University Press, New York, NY) p 248.
3. Moritz C & Agudo R (2013) The future of species under climate change: resilience or decline? *Science* 341(6145):504-508.
4. Hoffmann AA & Sgrò CM (2011) Climate change and evolutionary adaptation. *Nature* 470:479-485.
5. Bradshaw WE & Holzapfel CM (2006) Climate change - Evolutionary response to rapid climate change. *Science* 312(5779):1477-1478.
6. Norberg J, Urban MC, Vellend M, Klausmeier CA, & Loeuille N (2012) Eco-evolutionary responses of biodiversity to climate change. *Nature Climate Change* 2(10):747-751.
7. Skelly DK, Joseph LN, Possingham HP, Freidenburg LK, Farrugia TJ, Kinnison MT, & Hendry AP (2007) Evolutionary responses to climate change. *Conservation Biology* 21(5):1353-1355.
8. Diffenbaugh NS & Field CB (2013) Changes in ecologically critical terrestrial climate conditions. *Science* 341(6145):486-492.
9. Starrfelt J & Kokko H (2012) Bet-hedging - a triple trade-off between means, variances and correlations. *Biological Reviews* 87(3):742-755.

10. West-Eberhard MJ (2003) *Developmental Plasticity and Evolution* (Oxford University Press, Oxford, UK).
11. Piersma T & Drent J (2003) Phenotypic flexibility and the evolution of organismal design. *Trends in Ecology & Evolution* 18(5):228-233.
12. Cleland EE, Chuine I, Menzel A, Mooney HA, & Schwartz MD (2007) Shifting plant phenology in response to global change. *Trends in Ecology & Evolution* 22(7):357-365.
13. Moran NA (1992) The evolutionary maintenance of alternative phenotypes. *American Naturalist* 139(5):971-989.
14. Schlichting CD & Pigliucci M (1998) *Phenotypic Evolution: A Reaction Norm Perspective* (Sinauer Associates Inc., Sunderland, Massachusetts) p 387.
15. Frank SA (2011) Natural selection. I. Variable environments and uncertain returns on investment. *Journal of Evolutionary Biology* 24(11):2299-2309.
16. Simons AM (2011) Modes of response to environmental change and the elusive empirical evidence for bet hedging. *Proc. R. Soc. B-Biol. Sci.* 278(1712):1601-1609.
17. Schwander T & Leimar O (2011) Genes as leaders and followers in evolution. *Trends in Ecology & Evolution* 26(3):143-151.
18. Roh K, Safaei FRP, Hespanha JP, & Proulx SR (2013) Evolution of transcription networks in response to temporal fluctuations. *Evolution* 67(4):1091-1104.
19. McNamara JM, Trimmer PC, Eriksson A, Marshall JAR, & Houston AI (2011) Environmental variability can select for optimism or pessimism. *Ecology Letters* 14(1):58-62.
20. Borjigin J, Zhang LS, & Calinescu AA (2012) Circadian regulation of pineal gland rhythmicity. *Mol. Cell. Endocrinol.* 349(1):13-19.
21. Boutin S, Wauters LA, McAdam AG, Humphries MM, Tosi G, & Dhondt AA (2006) Anticipatory reproduction and population growth in seed predators. *Science* 314(5807):1928-1930.
22. Gabriel W (2006) Selective advantage of irreversible and reversible phenotypic plasticity. *Archiv Fur Hydrobiologie* 167(1-4):1-20.
23. Fischer B, Taborsky B, & Kokko H (2011) How to balance the offspring quality-quantity tradeoff when environmental cues are unreliable. *Oikos* 120(2):258-270.
24. Hainsworth FR & Wolf LL (1970) Regulation of oxygen consumption and body temperature during torpor in a hummingbird, *Eulampis jugularis*. *Science* 168(3929):368-369.
25. Geiser F (2013) Hibernation. *Current Biology* 23(5):R188-R193.
26. Mills LS (2013) Camouflage mismatch in seasonal coat color due to decreased snow. *Proceedings of the National Academy of Sciences of the United States Of* 110(18):7360-7365.
27. Lefebvre L, Reader SM, & Sol D (2004) Brains, innovations and evolution in birds and primates. *Brain Behavior and Evolution* 63(4):233-246.
28. Dunlap AS & Stephens DW (2009) Components of change in the evolution of learning and unlearned preference. *Proc. R. Soc. B-Biol. Sci.* 276(1670):3201-3208.
29. Sol D (2009) The cognitive-buffer hypothesis for the evolution of large brains. *Cognitive ecology II*, eds Dukas R & Ratcliffe JM (The University of Chicago Press, Chicago, IL), pp 111-134.
30. Botero CA, Boogert NJ, Vehrencamp SL, & Lovette IJ (2009) Climatic Patterns Predict the Elaboration of Song Displays in Mockingbirds. *Current Biology* 19(13):1151-1155.

31. Tollrian R (1990) Predator-induced helmet formation in *Daphnia cucullata* (SARS). *Archiv Fur Hydrobiologie* 119(2):191-196.
32. Rubenstein DR (2011) Spatiotemporal environmental variation, risk aversion, and the evolution of cooperative breeding as a bet-hedging strategy. *Proceedings of the National Academy of Sciences* 108(Supplement 2):10816-10822.
33. Crean AJ & Marshall DJ (2009) Coping with environmental uncertainty: dynamic bet hedging as a maternal effect. *Philosophical Transactions of the Royal Society B* 364:1087-1096.
34. van der Woude M (1996) Epigenetic phase variation of the pap operon in *Escherichia coli*. *Trends in Microbiology* 4(1):5-9.
35. Both C & te Marvelde L (2007) Climate change and timing of avian breeding and migration throughout Europe. *Climate Research* 35:93-105.
36. deMenocal PB (2011) Climate and human evolution. *Science* 331:540-542.
37. Scheffer M (2010) Complex systems: foreseeing tipping points. *Nature* 467(7314):411-412.
38. Diaz Arenas C & Cooper TF (2013) Mechanisms and selection of evolvability: experimental evidence. *FEMS Microbiology Reviews* 37(4):572-582.

Acknowledgments: C.A.B. was supported by USGS Grant/Cooperative Agreement # G10AC00624. J.W. was supported by the CBD/NTNU. D.R.R. was supported by NSF (IOS-1121435 and IOS-1257530).

485 **Figure legends**

486

487 **Fig. 1.** Effects of environmental stochasticity on the evolution of thermal strategies when
488 environments are either completely unpredictable ($P = 0$) or completely predictable ($P = 1$).
489 Stochastic environmental variation (top panels) was modeled by setting the value of weighting
490 constants to $A = 0$ and $B = 1$. Conversely, comparable deterministic variation (bottom panels)
491 was modeled through $A = 1$, $B = 0$ and $R = 1$. The norm of reaction plots depict the strategies of
492 5,000 individuals at generation 50,000 in representative replicate simulation runs. Darker colors
493 indicate that a higher number of individuals share a given response to a particular environmental
494 cue. Comparison of the top and bottom panels indicates that the way in which environments vary
495 – stochastically versus deterministically – is less important to evolution than the degree to which
496 individuals can anticipate such variation.

497

498 **Fig. 2.** Evolutionary response to environmental variation under different levels of predictability
499 (P) and relative timescale of environmental variation (R). At each parameter combination in (**A**),
500 the 100 mean population reaction norms that evolved at generation 50,000 in different replicate
501 simulations are depicted as in Fig. 1 with environmental cues on the x-axis and the resulting
502 insulation phenotypes on the y-axis (labels omitted for simplicity). If only one reaction norm is
503 visible, this is an indication that the same response evolved in all replicates. As illustrated in
504 panel (**C**), reaction norms are depicted in black when $\bar{s} \leq 0.5$ (see Table S1 for details). In such a
505 case, phenotypic plasticity does not occur (a is not expressed) and the reaction norm is flat. In
506 case of a plastic response ($\bar{s} > 0.5$), reaction norms are depicted in a color gradient ranging from
507 red when $\bar{a} = 1$ (reversible plasticity) to blue when $\bar{a} = 0$ (irreversible plasticity). For simplicity,

508 secondary reaction norms are depicted in green with intensity proportional to how often they are
509 used (i.e., they are not visible if $\bar{h} = 1$). (**B**) The consistency of outcomes across replicates in
510 panel (**A**) suggests that different regions in parameter space favor different modes of response.
511 'Conservative' and 'diversifying' bet-hedging are identified in panel (**B**) as CBH and DBH,
512 respectively. Dashed grey lines in panel (**B**) depict changes in the boundaries between different
513 adaptive regions when adjustment costs, k_a, are doubled from 0.01 to 0.02, and solid grey lines
514 depict changes when the cost of development, k_d, is doubled from 0.02 to 0.04.

515

516 **Fig. 3.** Adaptive tracking versus conservative bet-hedging in highly unpredictable environments
517 (here $P = 0$). Environmental cycles are depicted in black and the mean population phenotypic
518 value of I_0 is depicted in red. The evolved norms of reaction at generations 250 (dashed lines)
519 and 1000 (continuous lines) are shown to the right of each plot. (**A**) When environments change
520 very slowly (here log $R = 3$), norms of reaction evolve accordingly through mutation and natural
521 selection, leading to phenotypic changes in the population over time. (**B**) In contrast, when
522 environments change very rapidly (here log $R = 0$), adaptive tracking is not possible and a
523 phenotype that matches the average value of environmental conditions (i.e., $I_0 \approx 0$) becomes
524 fixed.

525

526 **Fig. 4.** Rates of extinction when transitioning into nearby regions of parameter space when $q =$
527 2.2. Each subplot within each panel depicts the baseline level of extinction at a given parameter
528 combination (inner square), and the extinction rates associated with transitioning into the nearest
529 parameter combination to the top, bottom, left and right of that cell (trapezoids). The boundaries
530 between response mode regions in Fig. 2B are presented as dashed lines. (**A**) We use a color

gradient from gray (0%) to red (100%) to depict absolute extinction rates (i.e., the proportion of simulations that went extinct during 100 replicate transition runs). (**B**) Relative rates were computed as (TR - BR) / BR, where TR = transition rate of extinction, and BR = baseline rate of extinction at the target parameter combination (i.e., where the population is moving into). The color scale for these rates ranges from blue (≤ -100%) to red (≥ 100%). The absence of blue trapezoids in (**B**) indicates that, in practice, transition rates were always similar or greater than their corresponding baselines.

Fig. 5. Representative examples of population dynamics during transitions through evolutionary tipping points in our model. (**A**) In the simulations depicted here, populations were forced to move from the region of reversible plasticity into that of bet-hedging by lowering P from 0.3 to 0.2 at log $R = 0$ (all other model parameters as in the main text). Top panels depict the change in the correlation between cues and environmental values, middle panels depict the evolution of traits before and after the transition (black = s, blue = a, green = h, gray = I_0, and red = b; the time of transition is depicted by a dashed vertical line at generation 5000), and bottom panels depict the associated changes in population size over time. (**A**) Even though the change in predictability is barely visible to the naked eye, populations immediately decline after predictability is reduced. (**B**) In most situations, populations become extinct because the mutations required to adapt to the new environment fail to arise. (**C**) However, in cases where beneficial mutations arise on time, these traits tend to reach fixation quickly and evolutionary rescue is complete.

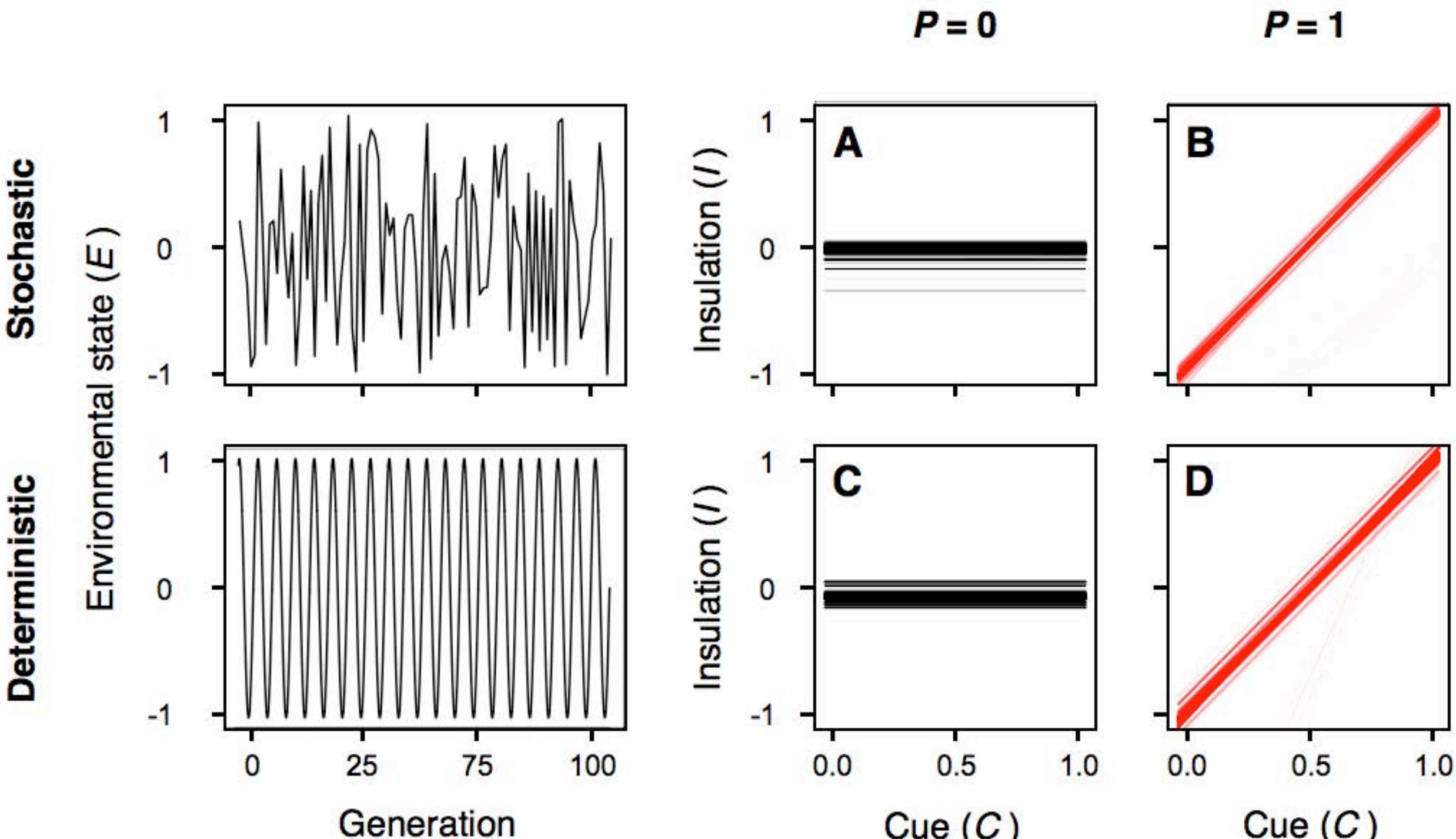
P = 0
P = 1
Stochastic
Deterministic
Environmental state (E)
Insulation (I)
A
B
C
D
1
0
-1
0
25
75
100
Generation
0.0
0.5
1.0
Cue (C)

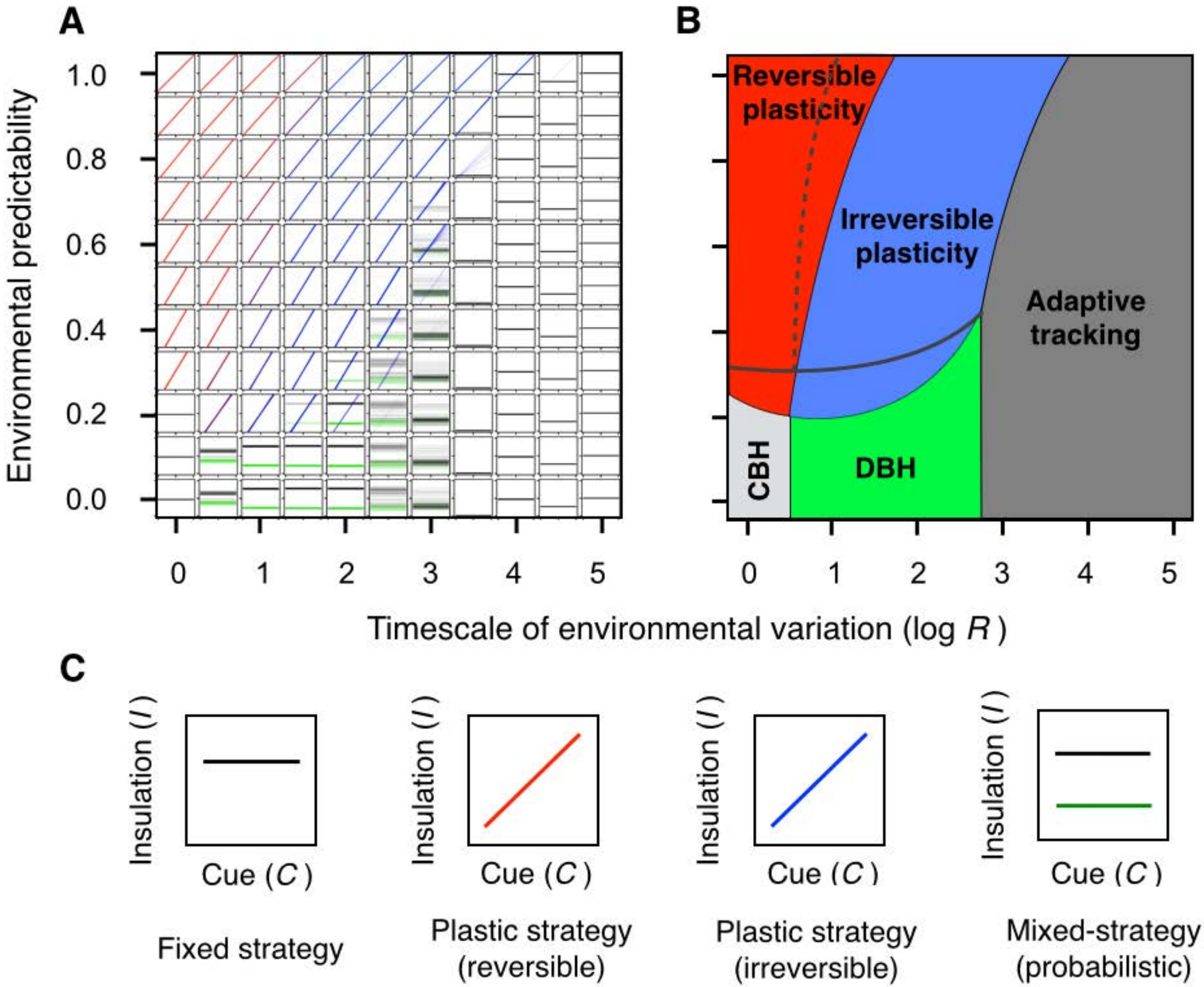
A
B
C
Environmental predictability
1.0
0.8
0.6
0.4
0.2
0.0
0
1
2
3
4
5
Reversible plasticity
Irreversible plasticity
Adaptive tracking
CBH
DBH
Timescale of environmental variation (log R)
Insulation (I)
Cue (C)
Fixed strategy
Plastic strategy (reversible)
Plastic strategy (irreversible)
Mixed-strategy (probabilistic)

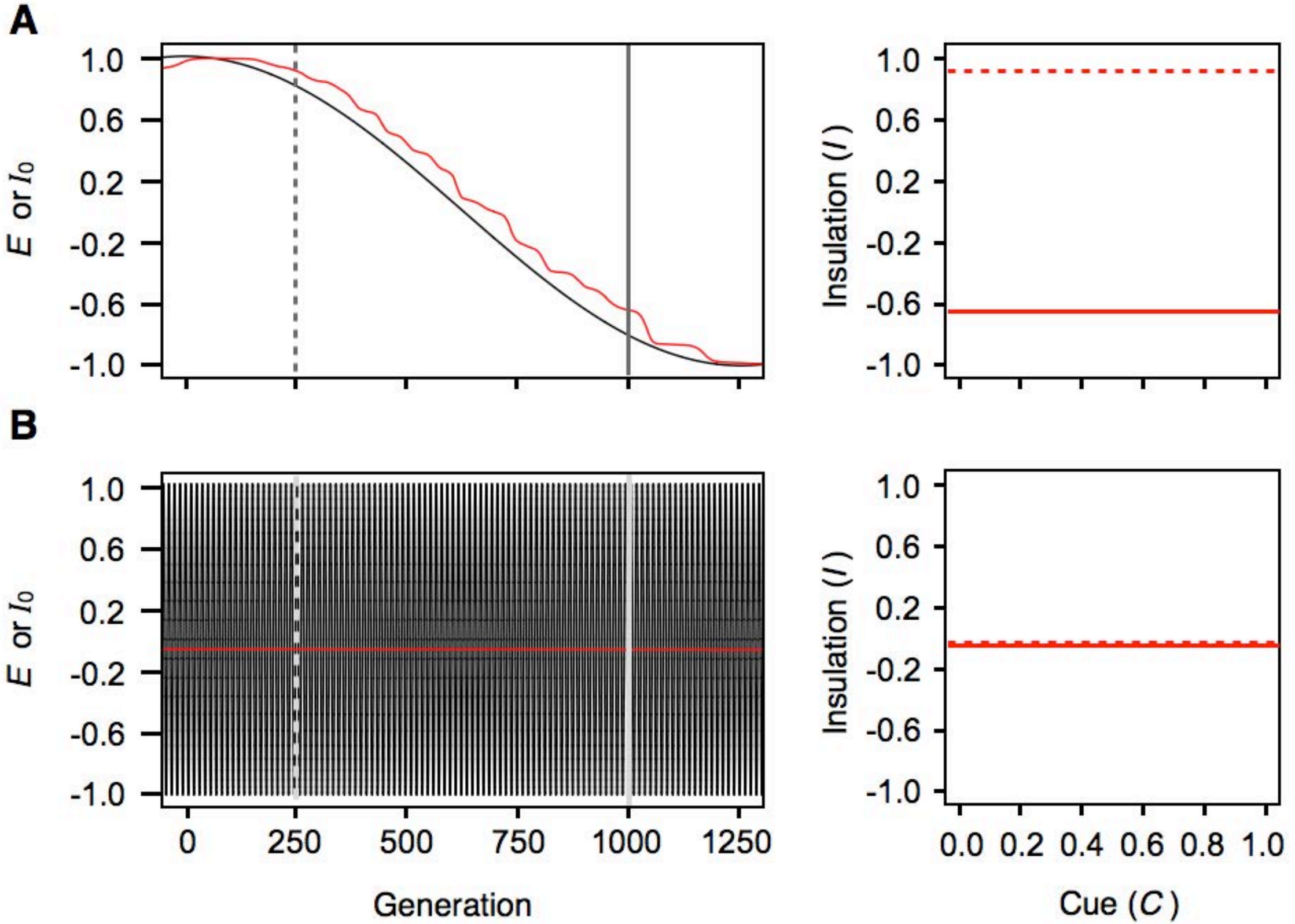
A
B
1.0
0.6
0.2
-0.2
-0.6
-1.0
E or I0
Insulation (I)
0
250
500
750
1000
1250
Generation
0.0
0.2
0.4
0.6
0.8
1.0
Cue (C)

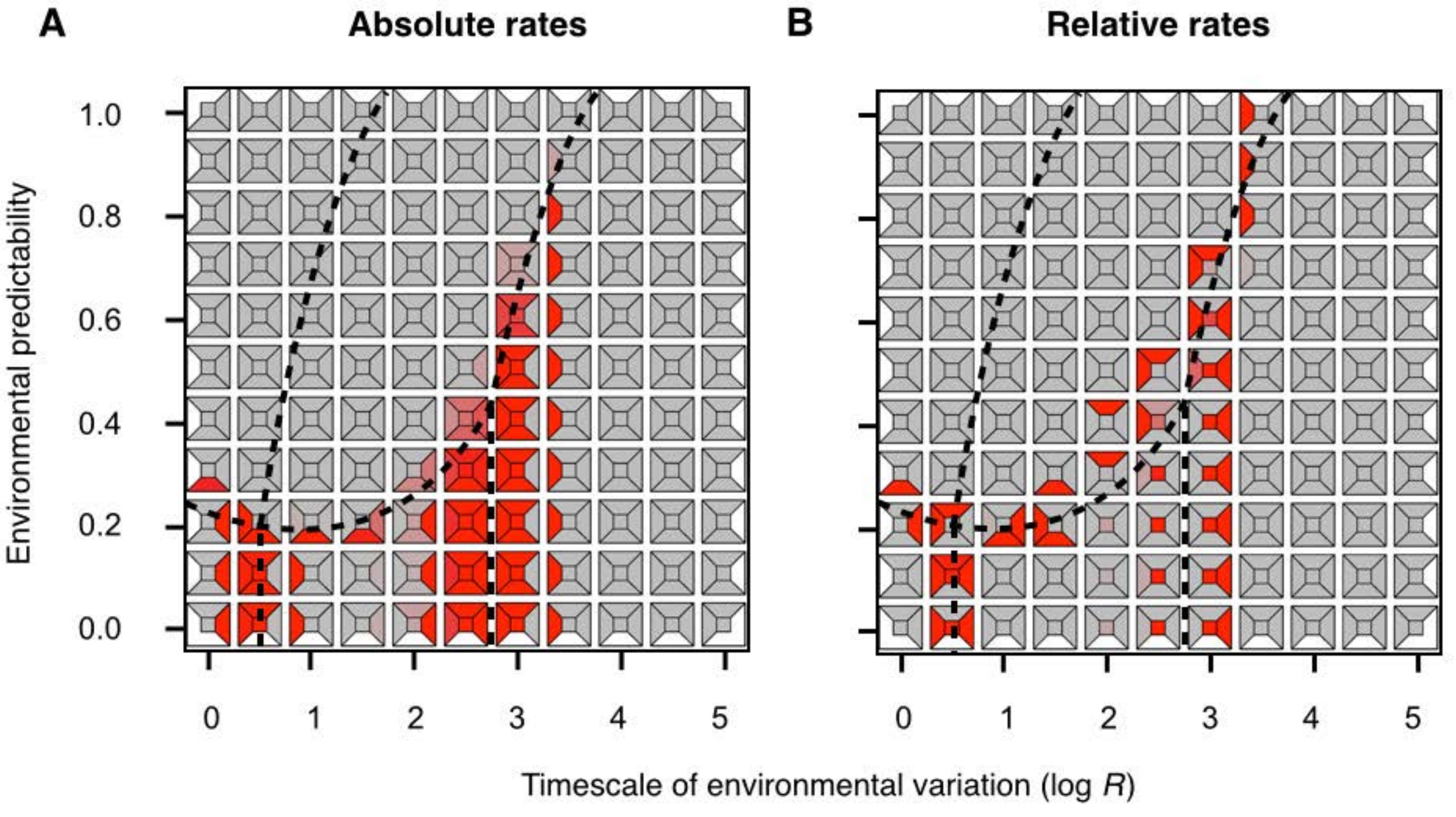
A
Absolute rates
B
Relative rates
Environmental predictability
1.0
0.8
0.6
0.4
0.2
0.0
0
1
2
3
4
5
0
1
2
3
4
5
Timescale of environmental variation (log R)

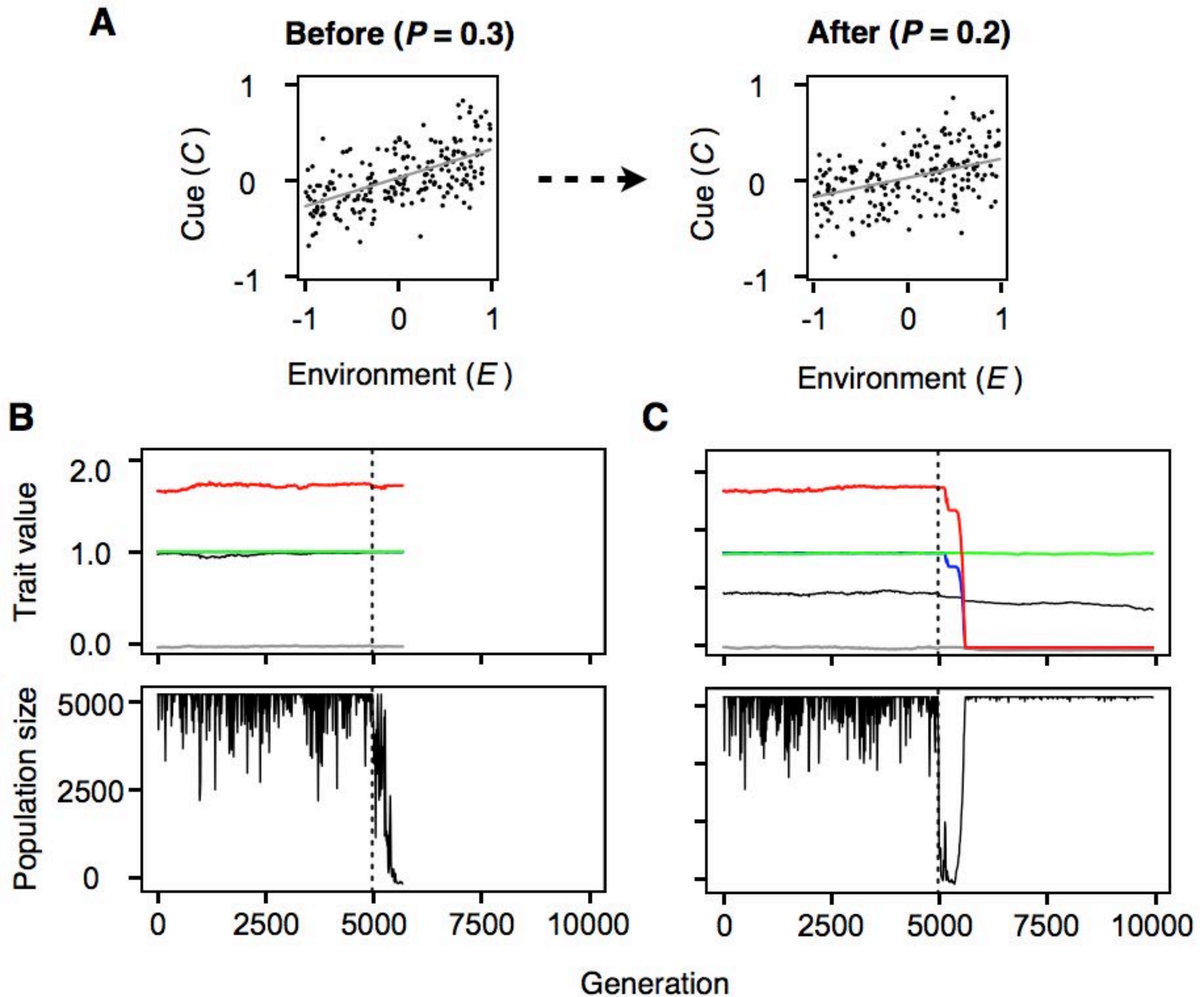
A
Before (P = 0.3)
After (P = 0.2)
Cue (C)
Environment (E)
1
0
-1
B
C
Trait value
2.0
1.0
0.0
Population size
5000
2500
0
0
2500
5000
7500
10000
Generation

Supporting Information Text

Evolutionary tipping points in the capacity to adapt to environmental change

Carlos A. Botero, Franz J. Weissing, Jonathan Wright and Dustin R. Rubenstein

Contents

1. *Modeling environmental predictability.*

Phenotypic plasticity relies on the ability to anticipate future environmental conditions. In many situations, this can be done by attending to environmental features that precede (and are correlated with) changes in relevant environmental parameters. For example, variation in day length tends to be well correlated with impending changes in temperature within temperate

regions, and changes in barometric pressure often forecast approaching storms, strong winds, and heavy rain. We refer to these anticipatory events as environmental 'cues' and model their information content by altering the degree to which they are correlated with future changes in the parameter of interest (i.e., temperature in our model). Thus, when cues are highly correlated with the parameter of interest we say that the environment is very predictable, and *vice versa*. We modeled environmental predictability, P, as a parameter that measures the correlation between cues, C, and environment, E, ranging from 0 (i.e., environmental cues contain no information on the potential future state of the environment) to 1 (i.e., environmental cues provide perfect information on the future state of the environment). Mathematically, environmental cues, C, are drawn in our model from a Gaussian distribution with mean,

$$\mu = P \cdot E ,$$

and standard deviation,

$$\sigma = (1 - P) / 3 ,$$

such that $C = E$ when $P = 1$, but C is uncorrelated with E when $P = 0$ (Fig. S1). Because 99.7% of the values in a normal distribution are contained within three standard deviations from the mean, dividing by three in the equation for sigma ensures that cues are primarily from the natural range of possible environmental values (i.e., [-1,1]). For example, at the extreme case with most variability—i.e., when $P = 0$—note that $\mu = 0$ and $3\sigma = 1$.

2. Genotypic variation within populations

In the main text we focus on population-level responses at 50,000 generations. However, we also investigated the patterns of genotypic variation within populations, because the same kind of

average outcome could be realized by either a genetically monomorphic or a genetically polymorphic population. Briefly, we observed that evolution consistently resulted in genetically monomorphic populations in our model (Fig. S2), even at the boundaries between response mode regions where average outcomes varied among replicates.

3. Evolutionary transitions when changes in environmental parameters lead to correlated changes in the genotype favored by selection

The highly consistent evolutionary outcomes observed in Fig. 2 indicate that the complex, multidimensional fitness landscape of our model tends to exhibit a single adaptive peak throughout most of parameter space. However, the evolution of different outcomes in different replicate simulations at the boundaries between response mode regions indicates that multiple adaptive peaks are likely to occur in the fitness landscape as selection shifts from favoring one outcome to another (Fig. S3).

4. Effects of alternative genotype-to-phenotype mapping and algorithms for selection

Our general findings are robust to alternative genotype-to-phenotype mapping schemes and to the consideration of evolutionary processes that may increase genetic variation within populations. Briefly, in all of the model variants that we have explored so far, we find that a single response mode has a clear selective advantage over all others at each parameter combination, and that, overall, the parameter space is divided into distinct response mode regions with relatively well-defined boundaries (Fig. S4).

To explore the effects of alternative genotype-to-phenotype mapping, we encoded norms of reaction as logistic rather than linear functions. In this model variant,

$$I = 2/\left(1+\exp\left(I_0 - b\cdot C\right)\right) - 1,$$

where I_0 and b are genetically inherited traits, and C is the current value of the environmental cue.

We also evaluated the robustness of our findings to processes that may increase genetic variation within populations by exploring the effects of density- and frequency-dependent selection. Negative density-dependent selection was implemented via the standard Beverton-Holt equation for population dynamics (1), where the total number of individuals in the next generation is a function of current population size. Thus, in the density dependent variant of our model, the number of offspring for individual i was drawn from a Poisson distribution with mean, $\mu = G\cdot W_i / W_{\max}$, where G is the *per capita* growth factor and W_{max} is the payoff an individual would accrue if it paid no costs and were able to match the exact temperature of its environment every time step of its life. The *per capita* growth factor, G, in this equation was computed as,

$$G = \beta/\left(1+\alpha\cdot N\right),$$

where α and β are constants (α = 0.00001 and β = 2 in Fig. S4C), and N is the current adult population size. To prevent unbounded population growth, excess offspring were selected at random and removed from the population whenever the new population size exceeded a carrying capacity of 5000 individuals.

In the model variant with frequency-dependent selection, W_i was weighted by the uniqueness of an individual's phenotype. Here, a rare-phenotype advantage was implemented by computing time step-specific payoffs as,

$$W_{i,t} = \exp\left(-\left|E_t - I_{i,t}\right| \cdot \tau\right) \cdot \left[1 - \exp\left(-\left|\bar{I} - I\right| \cdot \phi\right)\right],$$

where I is the mean insulation phenotype for the entire population, $I_{i,t}$ is the insulation phenotype of individual i at time step t, and ϕ is a constant that determines how strongly fitness improves for more unique individual insulation values ($\tau = 2$ and $\phi = 2$ in Fig. S4D). The cumulative payoff, W_i, for individual i in this model variant was then computed as the sum total of payoffs throughout its lifetime minus any costs of phenotypic adjustment. Thus,

$$W_i = \sum_{t=0}^{L} W_{i,t} \ ,$$

for non-plastic individuals, and

$$W_i = \sum_{t=0}^{L} W_{i,t} - k_d - n \cdot k_a \ ,$$

for plastic individuals.

5. Effects of variation in maximal fecundity on extinction rates after environmental change

Fig. S5 depicts the potential for extinction at each parameter combination (inner squares) as well as during transitions between adjacent combinations in parameter space for different values of q — i.e., the average number of offspring that an individual produces when it pays no plasticity costs and is able to exactly match its environment at every time step of its life. When reproductive output is low (smaller q), a major component of extinction during transition is

related to the high baseline levels of extinction when moving into environments that vary quickly and are fairly unpredictable. As q increases, baseline levels of extinction are radically reduced. However, the challenges of restructuring the genome in order to achieve a new optimum remain whenever crossing into a new response mode region.

6. Interpreting model results in the context of global climate change

Our model investigates evolutionary responses to any type of change in the characteristics of the environment, irrespective of scale and causes. However, in this section we provide a non-technical overview of how our model may apply, in particular, to the highly relevant context of global environmental change. The recent past has seen an unparalleled and rapid rise in mean temperatures and sea levels around the globe, as well as a corresponding increase in the frequency and unpredictability of extreme weather events (2-5). Our model addresses these potential environmental changes in the following ways:

6.1. Rapid change in mean environmental conditions: Earth's climate exhibits multiple types of oscillations, each of which operates at different timescales. For example, in addition to the yearly changes in precipitation and temperature that define our seasons, quasi-periodic phenomena like the El Niño/Southern Oscillation can influence environmental conditions and change the intensity of climatic extremes every 2-7 years (6). Similarly, temporal variation in Earth's orbit around the sun can lead to gradual changes in mean environmental parameters on much longer timescales, ultimately resulting in phenomena like the glacial and interglacial periods (7). We have become increasingly aware in recent years that anthropogenic activity has resulted in the

changes to these underlying environmental cycles (2, 6). Our model allows us to explore the effects of such disturbances through changes in the parameter that controls the relative timescale of variation, *R*. In the main text we define *R* as the number of environmental oscillations per lifespan. Thus, to study the potential effects of speeding up the rate at which environmental conditions vary, we can evaluate how populations respond when transitioning into regions of parameter space with lower *R*. When considering the potential effects of a given environmental change, we emphasize that *R* is a relative index, and that as such, its value will depend on lifespan. For example, while environments that change at a rate of 1°C/year can be approximated by a large *R* when considering short-lived organisms like bacteria, they are better characterized as low *R* when considering long-lived organisms like elephants or *Sequoia* trees. In other words, a given change in environmental cycles can potentially have very different consequences on species with different lifespans. Additionally, given that shorter lifespans increase the value of *R*, our model can inform us on the potential consequences of global-change-related reductions in lifespan (e.g., (8)) by exploring how populations respond to transitions into regions with higher *R* values.

6.2. Changes in the frequency and predictability of extreme weather events: It may be tempting to believe that because environmental changes are approximated in our evolutionary simulations as simple sinusoidal cycles, the 'world' is always somewhat predictable to our virtual individuals. That, however, is not the case and therefore we emphasize again that there is an important distinction between *the way* that environments vary and *how predictable* that variation is. As demonstrated in the main text, when there is no information regarding the phase of the cycle that the environment is currently at, the manner in which environments vary is completely

irrelevant to evolution (i.e., adaptive outcomes are identical whether we model environmental change as a series of stochastic events — $A = 0$, $B = 1$, and therefore, $E_t = \varepsilon$ — or as simple sinusoidal cycles — $A = 1$, $B = 0$, and therefore, $E_t = \sin(2\pi t/LR)$). Thus, to explore the consequences of the increasing unpredictability of local environments in the context of climate change, we do not need to model increasingly irregular environmental cycles, but rather to alter the amount of information provided to individuals about the future states of their environment. In addition, by decoupling predictability from variability, our model provides important insights into the different effects of *faster* environmental change and more *unpredictable* conditions, both independently and in combination. Some insightful examples of how researchers have identified the use of informative environmental cues in natural systems that have evolved because of their tight correlation with future environmental conditions include work on hares (9), gulls (10), and jays (11).

7. SI Figure legends

Fig. S1. Effect of predictability, P, on the statistical association between cues, C, and environmental temperatures, E, in our model. Plots depict cues derived from 200 randomly selected values of E when (A) $P = 1$, (B) $P = 0.5$, and (C) $P = 0$.

Fig. S2. Among- and within-replicate variation evolved in our model at generation 50,000. Norms of reaction are depicted as in Fig. 2 in the main text, with environmental cues on the x-axis and the resulting insulation phenotype on the y-axis (labels omitted for simplicity). (**A**) Variation among replicates is depicted by plotting the average reaction norms for each of 100

independent replicate simulation runs (same as Fig. 2A). (**B**) Variation within replicates is depicted by plotting the reaction norms for each of 5,000 individuals from one representative example at each parameter combination. As in the main text, primary reaction norms are plotted in black ($s \leq 0.5$) or in a color gradient from blue ($s > 0.5$, $a = 0$) to red ($s > 0.5$, $a = 1$), and secondary reaction norms are plotted in green with more intense colors indicating that a greater number of populations or individuals share a particular response. Importantly, the coexistence of different response modes within a replicate occurs primarily at the boundaries between adjacent response mode regions.

Fig. S3. Fitness landscapes illustrating the emergence of evolutionary tipping points. (**A**) Plots depicting the change of an idealized one-dimensional fitness landscape with an environmental parameter like R or P. Genotypes corresponding to different adaptive response modes are depicted in different colors. For most values of the environmental parameter, the fitness landscape exhibits a single adaptive peak, leading to a consistent evolutionary outcome in all replicate simulations. Changes in the environmental parameter correspond to (relatively small) shifts in the location of the adaptive peak, which can relatively easily be tracked by adaptive evolution. However, when the environmental parameter approaches a value corresponding to a boundary between two response mode regions, the landscape exhibits multiple adaptive peaks (middle plot in top panel), and evolutionary outcomes can therefore vary among replicate simulations. A further change in the environmental parameter corresponds to the disappearance of the earlier fitness peak, necessitating the rapid evolution to the new fitness peak that may be separated from the earlier peak by a large distance in genotype space. The hysteresis plot in (**B**) depicts this situation for $R = 100$ generations per environmental cycle—i.e., $\log(R) = 2$ in Fig. 2

of the main text—(cbh = conservative bet hedging; dbh = diversifying bet-hedging; ip = irreversible plasticity; rp = reversible plasticity; at = adaptive tracking). At low predictability values we observe only the evolution of diversifying bet-hedging, whereas at high values we see only the evolution of irreversible (or developmental) plasticity. However, close to the boundary between these regions (depicted here in gray) we see that replicates can result in either one of these evolutionary outcomes.

Fig. S4. Mean evolutionary outcomes at generation 50,000 for different parameter combinations under different model assumptions. (**A**) Reaction norms evolved under the baseline model described in the main text (same as depicted in Fig. 2). (**B**) Reaction norms evolved under the model variant with alternative genotype-to-phenotype mapping (i.e., reaction norms encoded as logistic rather than linear functions). (**C**) Reaction norms evolved under the model variant with negative density-dependent selection implemented through Beverton-Holt population dynamics. (**D**) Reaction norms evolved under the model variant with negative frequency-dependent selection implemented through a rare phenotype advantage. Ten replicate simulations are depicted per subplot in panels (**B-C**) and 100 replicates per subplot are depicted in (**A**). Note that similar response mode regions are observable across the different model variants.

Fig. S5. Effects of reproductive potential on relative rates of extinction during transition into a new set of environmental parameters. Each subplot within each panel depicts the baseline level of extinction at a given parameter combination (inner square), and the relative extinction rates (see main text for details) associated with transitioning into the nearest parameter combination to the top, bottom, left and right of that cell (trapezoids). Colors depict the gradient of extinction

from 0% (gray) to ≥100% (red). For comparison purposes, the boundaries between response mode regions in Fig. 2B are presented as dashed lines. When reproductive output is low (smaller q, panels **A** and **B**), a major component of extinction during transition is related to the high baseline levels of extinction when moving into environments that vary quickly and are fairly unpredictable. As q increases (panels **C** and **D**), the baseline levels of extinction decrease considerably throughout parameter space but the challenges of restructuring the genome in order to achieve a new optimum remain whenever crossing into new response mode regions.

References

1. Beverton RJH & Holt SJ (1957) On the dynamics of exploited fish populations. *Fishery Investigations Series II Volume XIX*, (U.K. Ministry of Agriculture, Fisheries, and Food, London, England).
2. Solomon S*, et al.* eds (2007) *Climate Change 2007: The Physical Science Basis* (Cambridge University Press, New York, NY).
3. Bradshaw WE & Holzapfel CM (2006) Climate change - Evolutionary response to rapid climate change. *Science* 312(5779):1477-1478.
4. Norberg J, Urban MC, Vellend M, Klausmeier CA, & Loeuille N (2012) Eco-evolutionary responses of biodiversity to climate change. *Nature Climate Change* 2(10):747-751.
5. Skelly DK*, et al.* (2007) Evolutionary responses to climate change. *Conservation Biology* 21(5):1353-1355.
6. Meehl GA*, et al.* (2000) Trends in extreme weather and climate events: Issues related to modeling extremes in projections of future climate change. *Bulletin of the American Meteorological Society* 81(3):427-436.
7. Hays JD, Imbrie J, & Shackleton NJ (1976) Variations in the Earth's Orbit: Pacemaker of the Ice Ages. *Science* 194(4270):1121–1132.
8. Munch SB & Salinas S (2009) Latitudinal variation in lifespan within species is explained by the metabolic theory of ecology. *Proceedings of the National Academy of Sciences* 106(33):13860-13864.
9. Mills LS*, et al.* (2013) Camouflage mismatch in seasonal coat color due to decreased snow. *Proceedings of the National Academy of Sciences of the United States Of* 110(18):7360-7365.
10. Brommer JE, Rattiste K, & Wilson AJ (2008) Exploring plasticity in the wild: laying date–temperature reaction norms in the common gull *Larus canus*. *Proc. R. Soc. B-Biol. Sci.* 275:687–693.
11. Ratikainen II & Wright J (2013) Adaptive management of body mass in Siberian jays. *Animal Behaviour* 85:427-434.

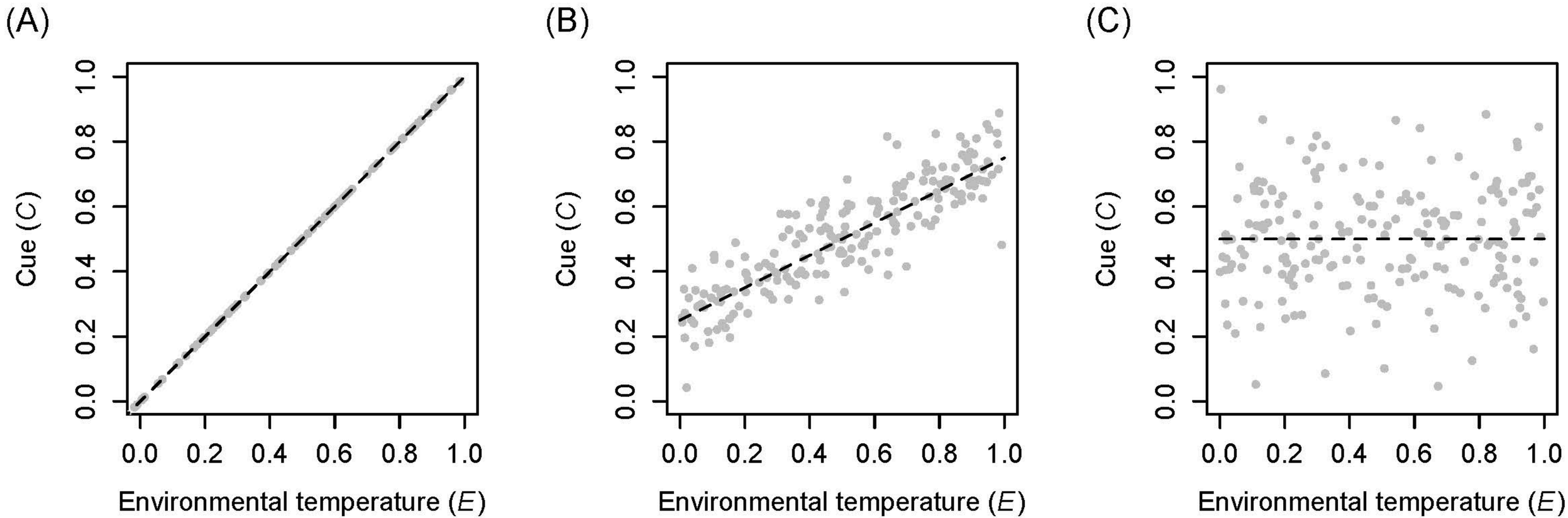
(A)
(B)
(C)
Cue (C)
Environmental temperature (E)
0.0
0.2
0.4
0.6
0.8
1.0

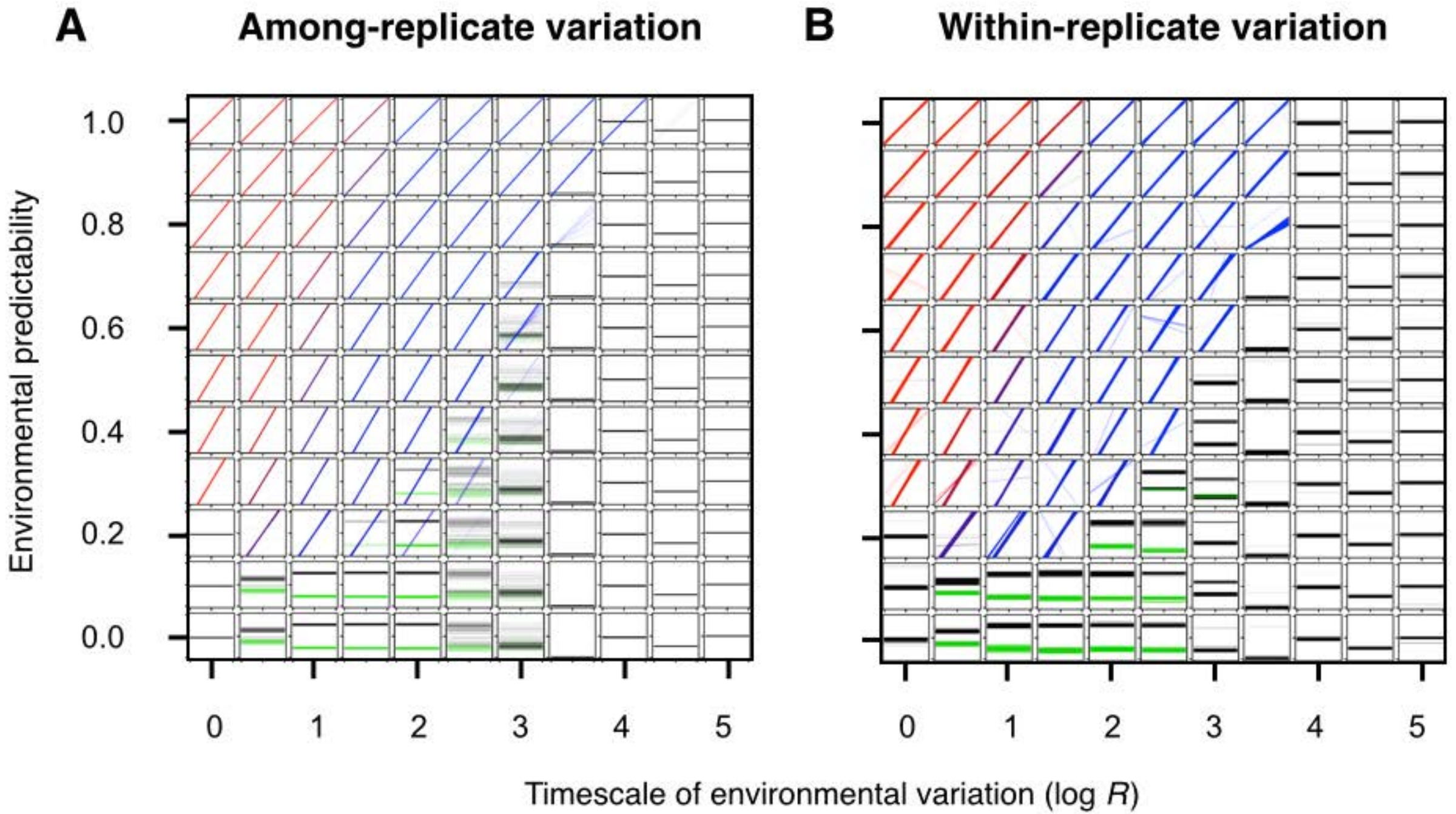
A
Among-replicate variation
B
Within-replicate variation
Environmental predictability
1.0
0.8
0.6
0.4
0.2
0.0
0
1
2
3
4
5
0
1
2
3
4
5
Timescale of environmental variation (log R)

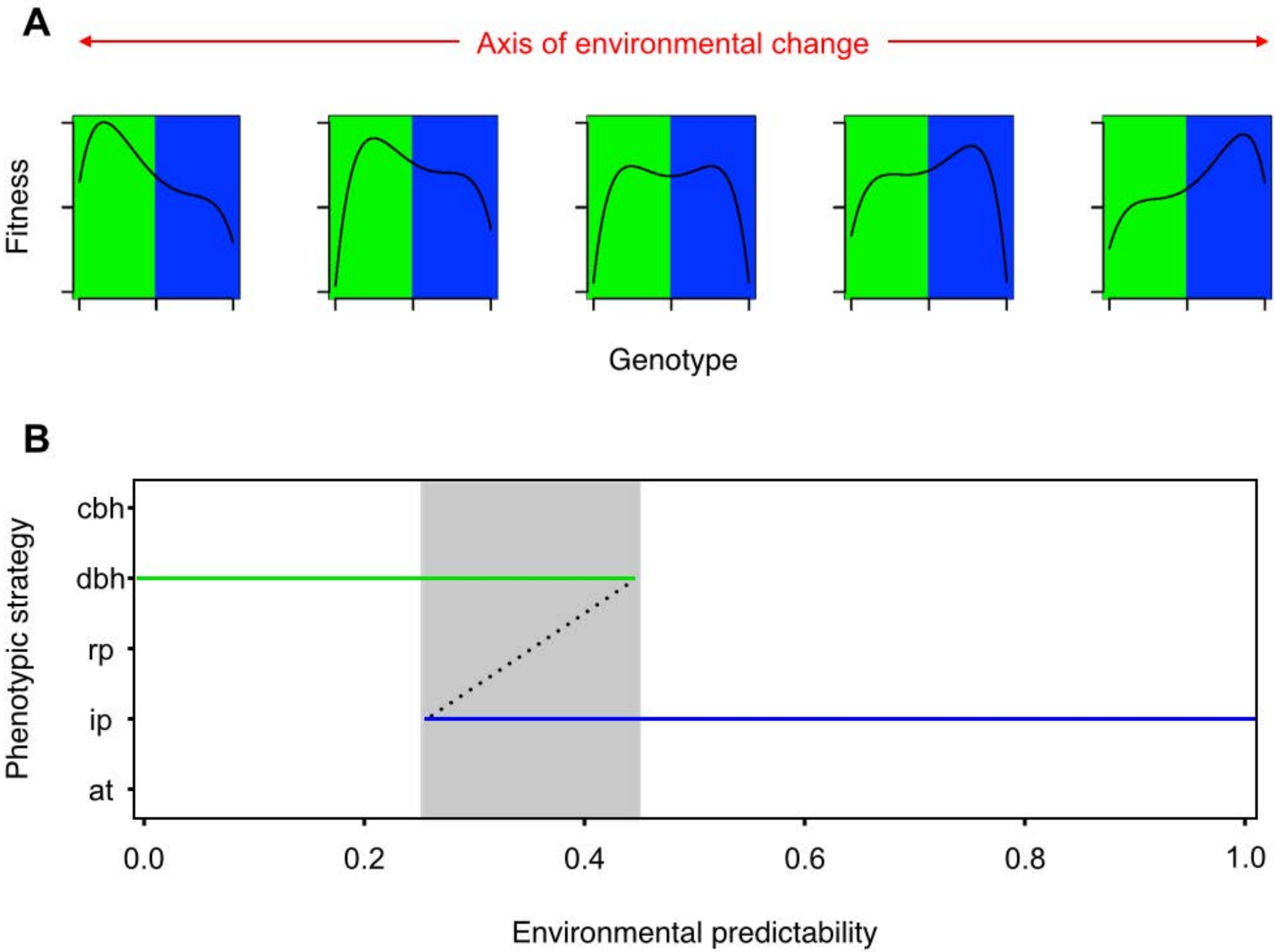
A
Axis of environmental change
Fitness
Genotype
B
Phenotypic strategy
cbh
dbh
rp
ip
at
0.0
0.2
0.4
0.6
0.8
1.0
Environmental predictability

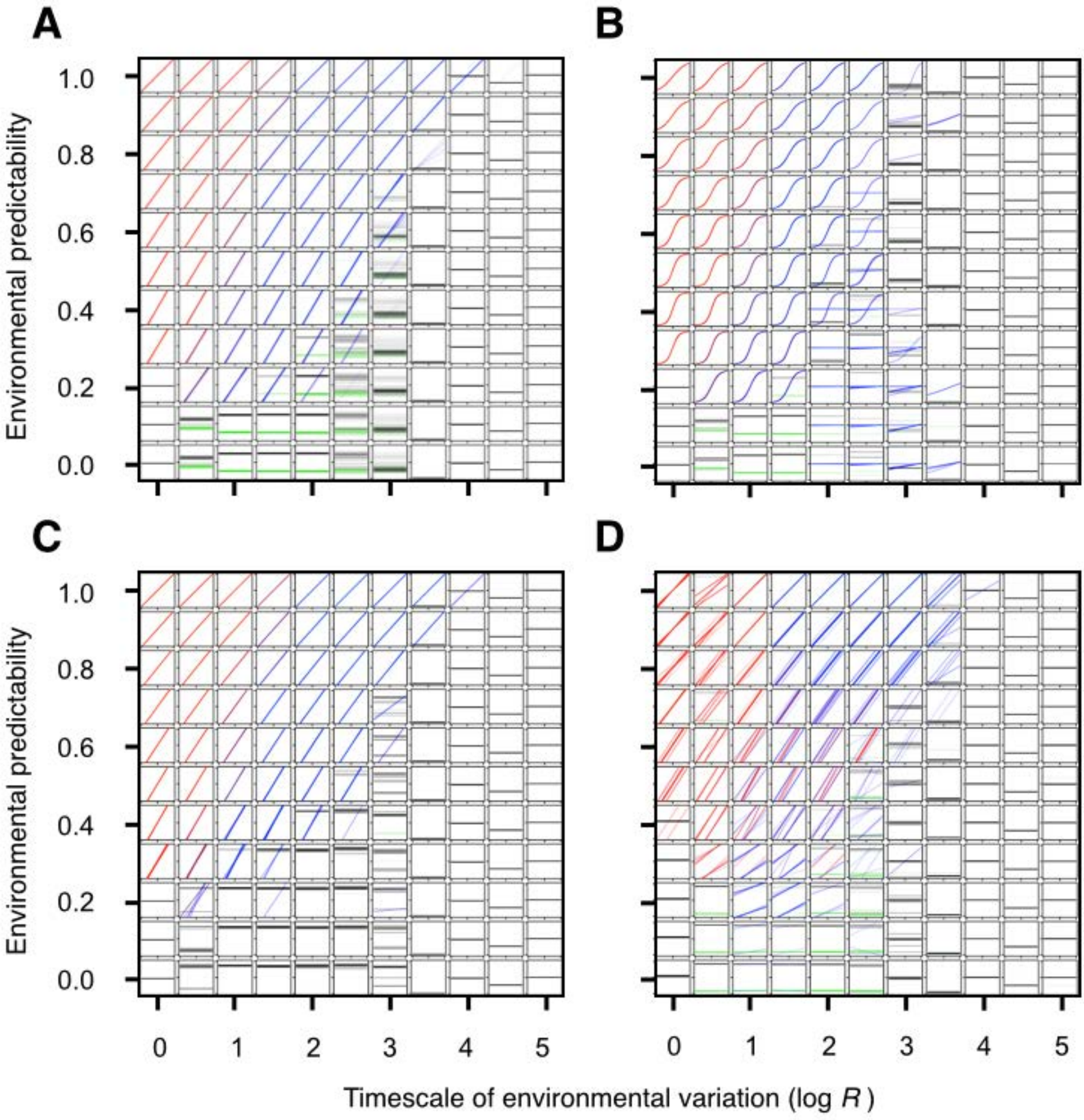
A
B
C
D
Environmental predictability
1.0
0.8
0.6
0.4
0.2
0.0
0
1
2
3
4
5
Timescale of environmental variation (log R)

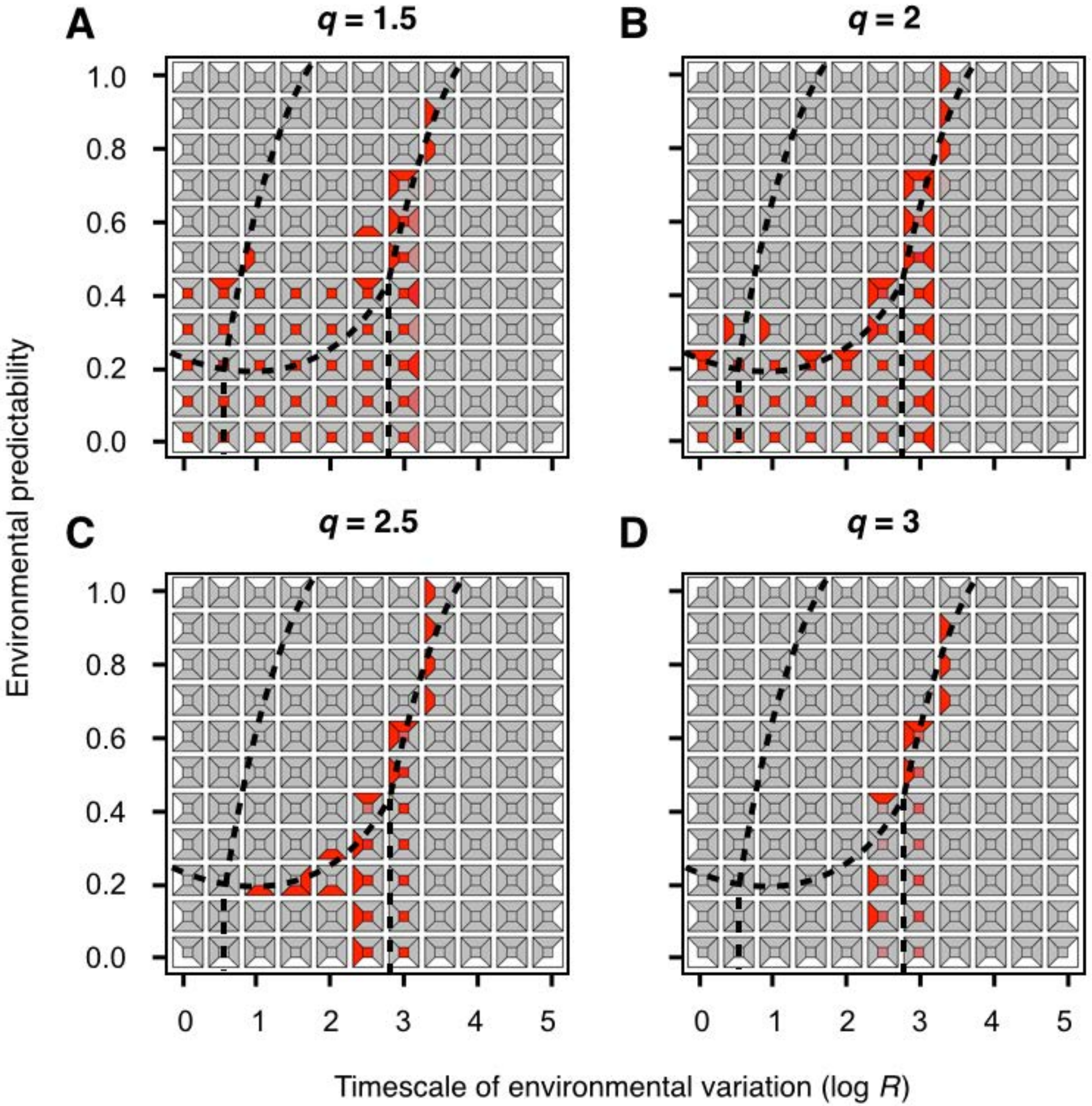
A
q = 1.5
B
q = 2
C
q = 2.5
D
q = 3
Environmental predictability
1.0
0.8
0.6
0.4
0.2
0.0
0
1
2
3
4
5
Timescale of environmental variation (log R)

Table S1. Phenotypic implications of the main reaction norms evolved in our model.

Reaction Norm	Phenotypic Implications
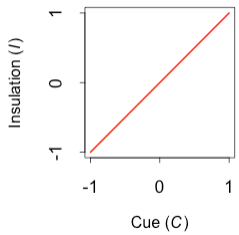	- Individuals produce more insulation at higher levels of the environmental cue ($s > 0.5$ and b or $b' \approx 1$). - Individuals adjust their phenotype every time step after development ($a \approx 1$). - Adaptive mode: REVERSIBLE PLASTICITY
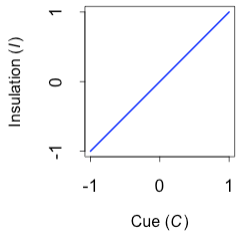	- Individuals produce more insulation at higher levels of the environmental cue ($s > 0.5$ and b or $b' \approx 1$). - Individuals are plastic during development but do not adjust their phenotype afterwards ($a \approx 0$). - Adaptive mode: IRREVERSIBLE PLASTICITY
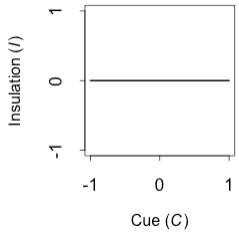	- Individuals produce a single, non-adjustable phenotype at all possible environmental cues ($s \leq 0.5$). - Adaptive mode: Single, fixed reaction norms occur in two contexts in our model (see Fig. 3 in main text for details): (i) in ADAPTIVE TRACKING, individual insulation levels closely match current environmental conditions, and mean population phenotypes vary gradually over time following the underlying environmental cycle; (ii) in CONSERVATIVE BET-HEDGING insulation levels are always approximately zero. Thus, although these individuals rarely ever match their current environmental conditions, they exhibit low variance in fitness by minimizing their average thermal mismatches over time.

Table S1. (Continued) Phenotypic implications of the main reaction norms evolved in our model.

Reaction Norm	Phenotypic Implications
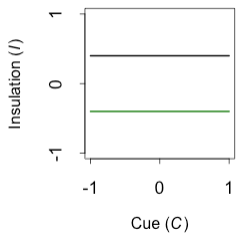	- Individuals produce a single, non-adjustable phenotype at all possible environmental cues ($s \leq 0.5$). - The phenotype depicted in black is produced with probability h and the one depicted in green is produced with probability $1-h$. - Adaptive mode: DIVERSIFICATION BET-HEDGING